

NARROW IRON K α LINES IN ACTIVE GALACTIC NUCLEI: EVOLVING POPULATIONS?

XIN-LIN ZHOU^{1,2} AND JIAN-MIN WANG^{1,2,3}
Accepted for Publication in The Astrophysical Journal Letters

ABSTRACT

We assemble a sample consisting of 66 active galactic nuclei (AGNs) from literature and the *XMM-Newton* archive in order to investigate the origin of the 6.4 keV narrow iron K α line (NIKAL). The X-ray Baldwin effect of the NIKAL is confirmed in this sample. We find the equivalent width (EW) of the NIKAL is more strongly inversely correlated with Eddington ratio (\mathcal{E}) than the 2-10 keV X-ray luminosity. Our sample favors the origin from the dusty torus and the X-ray Baldwin effect is caused by the changing opening angle of the dusty torus. The relation $EW - \mathcal{E}$ can be derived from a toy model of the dusty torus. If the unification scheme is valid in all AGNs, we can derive the Baldwin effect from the fraction of type II AGNs to the total population given by *Chandra* and *Hubble* deep surveys. Thus the evolution of populations could be reflected by the NIKAL's Baldwin effect.

Subject headings: galaxies: active - line: profile - X-rays: spectra

1. INTRODUCTION

Recent observations by *Chandra* and *XMM-Newton* have revealed that a narrow iron K α line (NIKAL) at 6.4 keV in the rest frame is a ubiquitous feature in AGN X-ray spectra. However, its origin is poorly understood.

There are two possible ways to test the origins of the NIKAL. Firstly, the full-width-half-maximum (FWHM) of the line may provide the motion of the emitting matter, indicating the location of the radiation region in the potential of the black hole at the center. The currently-available highest spectral resolution of *Chandra* is $\sim 1860 \text{ km s}^{-1}$ (FWHM) at 6.4 keV and *XMM-Newton* has a resolution of $\sim 7200 \text{ km s}^{-1}$ at the same energies. There are a dozen of objects which have been resolved by *Chandra* and *XMM-Newton*, e.g. $\sim 1780_{-1220}^{+1420} \text{ km s}^{-1}$ in NGC 5548; $\sim 1700_{-390}^{+410} \text{ km s}^{-1}$ in NGC 3783 (Yaqoob et al. 2004). However, the current observational data set up less constraint on the NIKAL's origin since they cover a range of $10^3 \sim 10^4 \text{ km s}^{-1}$ and the error bars are quite large.

Secondly, the variabilities of the NIKAL are expected to apply to test its origin. However, it appears rather constant and lacks the response to the changes in the continuum flux, for example, MCG-6-30-15 (Wilms et al. 2001, Lee et al. 2002), Mrk 6 (Immler et al. 2003), NGC 4051 (Pounds et al. 2004) and NGC 4593 (Reynolds et al. 2004). In our present sample, only Mrk 841 shows a rapid variation of the NIKAL with a timescale of 10 hours or less whereas the X-ray continuum is constant (Petrucci et al. 2002). The available data implies a rather constant geometry of the NIKAL's emission region.

Despite of the illusive properties of the NIKAL, there is an anti-correlation between the equivalent width (EW) of the NIKAL and X-ray continuum, namely, the X-ray Baldwin effect (Iwasawa & Taniguchi 1993, Nandra et al. 1997). This is recently confirmed in the *XMM-Newton* data by Page et al. (2004, hereafter P04). They argue that the origin of the NIKAL from BLR is not favored by: (1) BLR could only account for the NIKAL with a EW of less than 40 eV (see also Yaqoob et al. 2001); (2) the lack of the correlation between the NIKAL and optical/UV parameters. However, the origin of the NIKAL from a dusty torus has been explored by Krolik & Kallman

(1987, hereafter KK87) and Krolik et al. (1994). If the NIKAL indeed originates from the dusty torus, its subtended solid angle is decisive to the observed EW of the NIKAL. This implies that the opening angle of the dusty torus could be indicated by the EW of the NIKAL. In turn, the evolution of the open angle of the dusty torus could be reflected by the X-ray Baldwin effect.

In this Letter, we test the origin of the NIKAL by revisiting the *XMM-Newton* data. We find that the NIKAL EW much more strongly depends on the Eddington ratio and the current data agrees with an origin of evolving dusty torus.

2. THE SAMPLE AND STATISTICAL PROPERTIES

We collect all the AGNs with observations of *XMM-Newton* from literature and find 66 objects listed in Tab. 1. In order to minimize systematic errors in the correlation analysis, we use only the results obtained in P04 who give the NIKAL of 51 of 66 objects. We analyze the PN data of the additional 15 objects from the *XMM-Newton* archive according to the model described in P04. The sample consists of 16 narrow line Seyfert 1 galaxies (NLS1), 18 broad line Seyfert 1 galaxies (BLS1), 32 quasars including 14 radio-loud (RL) quasars. The redshift range of the present sample is $z = 0.002 - 3.4$, but only 7 objects have $z > 0.5$.

The black-hole masses (M_{BH}) are directly taken from the results of the reverberation mapping measurements of Peterson et al. (2004), or estimated from the empirical reverberation relation (Kaspi et al. 2000; hereafter K00), $M_{\text{BH}}/M_{\odot} = 4.82 \times 10^6 [\lambda L_{\lambda,44}(5100\text{\AA})]^{0.7} V_3^2$, where $\lambda L_{\lambda,44}(5100\text{\AA}) = \lambda L_{\lambda}(5100\text{\AA})/10^{44} \text{ erg s}^{-1}$ and $V_3 = \text{FWHM}(\text{H}\beta)/10^3 \text{ km s}^{-1}$. The values of $L_{\lambda}(5100\text{\AA})$ are taken from Vestergaard (2002) and Grupe et al. (2004), or calculated from the absolute magnitude in the B band of M_B given by Marziani et al. (2003) and Véron-Cetty et al. (2003) through an extrapolation of a power-law spectrum as $F_{\nu} \propto \nu^{-0.5}$. Additionally, 4 objects in the present sample are estimated via different methods, including 2 high-redshift quasars, 2 Seyfert 1.9. Only 57 of 66 objects have enough data to estimate the BH masses. We estimate bolometric luminosity for the Eddington ratio from $L_{\text{Bol}} = 9\lambda L_{\lambda}(5100\text{\AA})$ (K00) and from published papers if it is given. We then have

¹ Laboratory for High Energy Astrophysics, Institute of High Energy Physics, Chinese Academy of Sciences, Beijing 100039, P.R. China, wangjm@mail.ihep.ac.cn

² Graduate School of Chinese Academy of Sciences, Beijing 100039, P.R. China

³ to whom should correspond

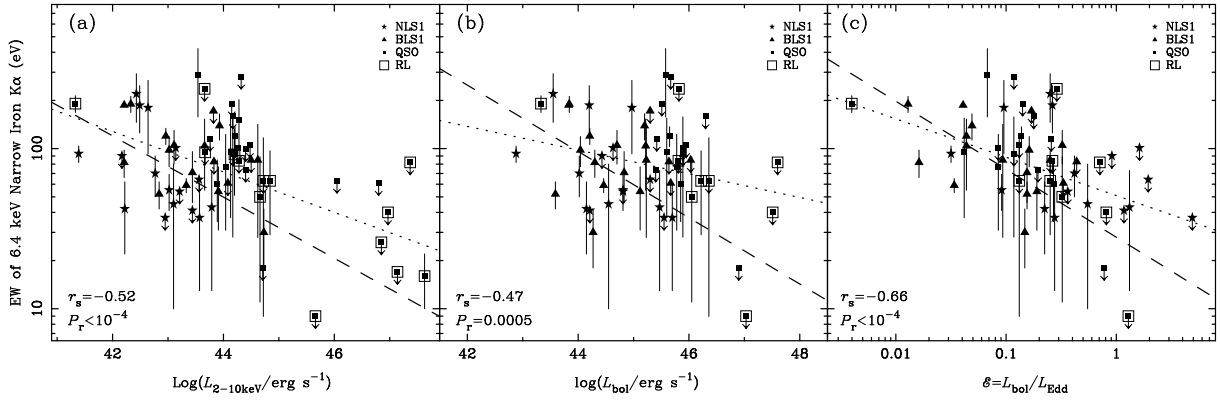


FIG. 1.— (a): the X-ray Baldwin effect; (b): the correlation of $EW-L_{\text{Bol}}$; (c): the strong anti-correlation of EW with Eddington ratio \mathcal{E} . The dashed lines indicates the relation for the entire dataset, dotted line without upper limits.

TABLE 1. THE *XMM-Newton* SAMPLE OF AGNs (SEE THE COMPLETE ELECTRONIC VERSION OF THE TABLE)

Name	z	Type	$\log L_{\text{Bol}}$	$H\beta$	$\log M_{\text{BH}}$	$\log \mathcal{E}$	Ref.	$\log L_X$	$EW_{\text{K}\alpha}$	Ref.		
(1)	(2)	(3)	(4)	(5)	(6)	(7)	(8)	(9)	(10)	(11)	(12)	(13)
1H 0707-495	0.0411	NLS1	44.43	R	1050	6.37	R	-0.04	11,13	42.17	< 90	1
1Zw 1 ^b	0.0611	NLS1	45.47	R	1240	7.25	R	0.12	3,13	43.79	34 ± 30	2

Table 2. The NIKAL EW correlation analysis

X	data	r_s	P_r	a	b
L_X	All	-0.52	$< 10^{-4}$	-0.19 ± 0.04	10.10 ± 1.49
	RQ only	-0.34	1.6×10^{-2}	-0.15 ± 0.05	8.51 ± 2.30
	Real	-0.38	2.8×10^{-2}	-0.13 ± 0.03	7.42 ± 1.47
L_{Bol}	All	-0.47	5.0×10^{-4}	-0.21 ± 0.05	11.10 ± 2.20
	RQ only	-0.36	1.1×10^{-2}	-0.15 ± 0.06	8.64 ± 2.58
	Real	-0.28	0.12	-0.07 ± 0.05	5.25 ± 2.25
\mathcal{E}	All	-0.66	$< 10^{-4}$	-0.42 ± 0.07	1.45 ± 0.08
	RQ only	-0.61	$< 10^{-4}$	-0.38 ± 0.08	1.52 ± 0.08
q	Real	-0.49	6.4×10^{-3}	-0.24 ± 0.07	1.71 ± 0.08

Note: $-\log EW = a \log X + b$

r_s is the Spearman's coefficient; P_r is the null probability.

the Eddington ratio $\mathcal{E} \equiv L_{\text{Bol}}/L_{\text{Edd}}$, where L_{Bol} is the bolometric luminosity and L_{Edd} is the Eddington luminosity. Throughout this paper, we use $H_0 = 75 \text{ km s}^{-1} \text{ Mpc}^{-1}$ and $q_0 = 0.5$.

Since the present sample includes upper limit data, we apply the Spearman's rank statistic and parameter EM (Expectation-Maximization) algorithm constructed by ASURV (Astronomy Survival Analysis; Isobe et al. 1986) package to the complete dataset for the correlation analysis. Table 2 gives the correlation analysis of the equivalent width with L_X , L_{Bol} and \mathcal{E} . Fig. 1 presents the plots of these correlations.

The X-ray Baldwin effect is confirmed by the present sample which is larger compared to P04. We find $EW \propto L_X^{-0.19 \pm 0.04}$ for the entire data. We have 16 NLS1s in our sample, which are frequently variable in X-ray. We thus explore the correlation between EW and the bolometric luminosity L_{Bol} . We find $EW-L_{\text{Bol}}$ is not better than $EW-L_X$ as shown in Fig. 1b and Table 2. Interestingly, we find a much stronger correlation of $EW \propto \mathcal{E}^{-0.42 \pm 0.07}$ for the entire sample as shown by Fig. 1c, indicating that the correlation of $EW-\mathcal{E}$ is more fundamental than $EW-L_X$. What does drive the correlations?

3. THE ORIGIN OF THE X-RAY BALDWIN EFFECT

The equivalent width of Fe K α line from the illuminated medium is given by KK87,

$$EW \approx \frac{E_{\text{K}\alpha}}{3+\Gamma} Y \left(\frac{\Delta\Omega}{4\pi} \right) \tau_{\text{K}}, \quad (1)$$

where $\tau_{\text{K}} \approx 0.7 f(\Xi) \mathcal{A}_{\text{Fe}} \tau_{\text{es}}$. Here is $E_{\text{K}\alpha} = 6.4 \text{ keV}$; Γ is the photon index of 2-10 keV band; Y is the photon production; $\Delta\Omega$ is the solid angle subtended by the illuminated matter; τ_{K} is the Fe K-edge optical depth; Ξ is the ionization parameter, $f(\Xi)$ is a weak function of Ξ , normalized as $f(30) = 1$ and f approaches 1.7 in the limit of small Ξ ; \mathcal{A}_{Fe} is the iron abundance in units of solar abundance; τ_{es} is the electron scattering optical depth.

P04 excludes the dependence of the NIKAL EW on the index Γ . Since we pay our attention to the NIKAL, the ionization parameter Ξ should be small enough and Y keeps a constant. The dependence of the NIKAL on Ξ and Y should be ruled out. The metallicity indicator (e.g., N V / C IV) measured from the BLR in quasars shows that the metallicity increases with luminosity (Hamann & Ferland 1993), and more strongly with the Eddington ratio (Shemmer et al. 2004). Such a dependence on the metallicity leads to an increases of the NIKAL EW with the Eddington ratio. This is just opposite to the present correlation shown by Fig 1c. Risaliti et al. (1999) find that the column density does not relate to the hard X-ray luminosity. This means that the Fe K edge depth can not result in the Baldwin effect. Iwasawa & Tanuguchi (1993) point out that the X-ray Baldwin effect may be caused by a changing covering factor similar to the optical Baldwin effect (Mushotzky & Ferland 1984), but they do not give more details.

3.1. Origin from Outer Region of Disk

The covering factor $\Delta\Omega/4\pi$ in Eq.1 is crucial to the EW of the NIKAL, implying the importance of geometry of the emission region. In the followings, we explore the probability that the NIKAL originates from the outer region of the accretion disk and the torus.

3.1.1. The outer region of the standard accretion disk

The solid angle subtended by the disk height can be derived from the standard accretion disk (Shakura & Sunyaev 1973)

$$\Delta\Omega \propto \frac{H}{R} \propto \begin{cases} \mathcal{E}^{3/20} & (P_{\text{gas}} \gg P_{\text{rad}}), \\ \mathcal{E} & (P_{\text{rad}} \gg P_{\text{gas}}), \end{cases} \quad (2)$$

where H is the half height of the disk at radius R from the center, P_{gas} and P_{rad} are the gas and radiation pressure, respectively. This directly indicates that the EW of iron $K\alpha$ line increases with the Eddington ratio, as $EW \propto \mathcal{E}^{3/20}$ or $EW \propto \mathcal{E}$. The correlation shown in Fig 1c rules out the origin of the NIKAL from outer region of the accretion disks.

For low Eddington ratios, the advection-dominated accretion flows (ADAF) can automatically switch on the standard disks at a radius larger than $10R_g$, where $R_g = 2GM_{\text{BH}}/c^2$ (Lu et al. 2004). For the slim disks, Chen & Wang (2004) show that they have structures similar to the standard disks beyond the photon trapping radius R_{tr} , where $R_{\text{tr}}/R_g = 720 (\dot{m}/50)$, $\dot{m} = \eta \dot{M} c^2 / L_{\text{Edd}}$ and $\eta = 0.1$ (Wang & Zhou 1999, Wang & Netzer 2003). Thus our discussions (eq. 2) are available for both kinds of the objects with low and high Eddington ratios, ruling out the possible origin from the outer region.

3.1.2. The self-gravity disk

The outer parts of the standard accretion disks tend to be self-gravity-dominated, Goodman et al. (2003) show

$$\Delta\Omega \propto \frac{H}{R} \propto \begin{cases} Q^{-5/3} \mathcal{E}^{1/3} & (\alpha \propto P_{\text{tot}}), \\ Q^{-6/7} \mathcal{E}^{2/3} & (\alpha \propto P_{\text{gas}}), \end{cases} \quad (3)$$

where Q is the Toomre stability parameter for Keplerian rotation, α is the viscosity and P_{tot} is the total pressure. We have $EW \propto \mathcal{E}^{1/3}$ or $EW \propto \mathcal{E}^{2/3}$. This shows that the NIKAL from a self-gravity-dominated disk will strengthen with \mathcal{E} . This origin is also ruled out by Fig 1c.

3.2. The dusty torus

The mid-infrared interferometry telescope reveals a geometrically and optically thick torus in the well-known Seyfert 2 galaxy NGC 1068 (Jaffe et al. 2004, hereafter). The torus has a thickness of $H/R > 0.6$ and a temperature of 800-1000 K for the inner shell, 300 K for outer shell, where H is the half height of torus at the distance R from its central engine. Such an unusual result provides direct support for the unified model (Antonucci 1993). The covering factor plays a key role in the unification scheme, but it is poorly understood. We employ the torus model to understand the X-ray Baldwin effect from two ways.

3.2.1. Covering factors of the tori and the accretion rates

Krolik & Begelman (1988) suggest that the obscuring matter takes the form of compressed molecular clouds. They derive the covering factor of the torus based on a toy model for cloud size distribution,

$$\mathcal{C} = \frac{1}{4} \left(\frac{\alpha}{\gamma} \right) \left(\frac{V_{\text{orb}}}{\Delta V} \right) \quad (4)$$

where the two parameters $\alpha \sim 1$ and $\gamma \sim 1$, V_{orb} is the orbital velocity of the clouds at radius R and $\Delta V^2 = \Delta V_z^2 + \Delta V_r^2 + \Delta V_\theta^2 \approx 3\Delta V_z^2$ is the square of the random velocity. The collisions due to the random motions of the clouds lead to an inflow to the central black hole with a mass rate of

$$\dot{M} = 1.5 V_{200} R_{\text{pc}} c^{-2} M_\odot \text{yr}^{-1}, \quad (5)$$

where $V_{200} = V_{\text{orb}}/200 \text{ km s}^{-1}$ and the radius of the inner edge of the torus $R_{\text{pc}} = R_t/1 \text{ pc}$. We thus have a relation of $\mathcal{C} \propto r_t^{1/4} \mathcal{E}^{-1/2}$, where $r_t = R_t/R_g$. The covering factor is insensitive to the inner radius (r_t) of the torus, but very sensitive to the Eddington ratio. We then have $EW \propto \mathcal{E}^{-0.5}$. This quite nicely matches the correlation $EW \propto \mathcal{E}^{-0.42 \pm 0.07}$ (in Table 2). This consistence shows an intrinsic relation between the accretion disk and the torus.

3.2.2. Type II AGN Populations

On the other hand, the covering factor of the torus can be derived from the statistics of the populations of AGNs in deep sky surveys if the unification scheme works for all AGNs. The deep survey data from *Chandra*, *Hubble* and others show that the population of type II AGNs is decreasing with X-ray luminosity (Ueda et al. 2003, Steffen et al. 2003, Hasinger 2003). This census indicates the changing of the opening angle in different individuals. Using the least square method, we fit the data in Fig 6b in Hasinger (2003) and obtain

$$\log P_{\text{II}} = (3.38 \pm 0.48) - (0.08 \pm 0.02) \log L_{2-10\text{keV}} \quad (6)$$

This relation shows that type II quasars will be rare among luminous quasars. This is consistent with the fact that the NIKAL disappears in luminous quasars. If the half-open angle of torus is θ , the solid angle of torus subtending the central engine is $\Delta\Omega/4\pi = \cos\theta = P_{\text{II}}$. This relation is based on assumption that the orientation of the torus is random in the sky. Inserting eq. (6) into (1) with the help of $\Delta\Omega/4\pi = \cos\theta = P_{\text{II}}$ and $\Gamma = 1.7$, we have

$$\log EW = (6.20 \pm 0.48) - (0.08 \pm 0.02) \log L_{2-10\text{keV}}. \quad (7)$$

We take $\tau_K = 1$, otherwise τ_K is too large for the fluorescence photons to escape whereas τ_K is too small to produce the NIKAL (Krolik et al. 1994; Levenson et al. 2002).

It is very interesting to note that this relation is consistent with the Baldwin effect described in Table 2. This suggests an *intrinsic* relation between the NIKAL Baldwin effect and evolution of the dusty torus. The fraction of type II AGNs in the deep surveys indicates that the increasing X-ray luminosity enlarges the opening angle of the dusty torus and lowers the covering factor of the dusty torus. Quantitative calculations of this process still lack in the literatures. In addition, the collisions among the molecular clouds result in an evolution of the torus covering factors and non-thermal emissions detectable in radio to sub-GeV γ -ray bands (Wang 2004). Though the explanation of $L_X - P_{\text{II}}$ relation remains open, the canonic evolutionary model of the dusty torus can be reflected by the X-ray Baldwin effect.

We should emphasize that the derived Baldwin effect is based on the deep survey results of *Chandra*, *Hubble*, etc., which is different from ours. Hence Eq. (7) is not self-consistent. Though the fraction P_{II} also depends on redshift (Steffen et al. 2003), most of the present sample are low-redshift AGNs, the dependence of P_{II} on the redshift can be ignored. If the survey data is available for iron $K\alpha$ line analysis, it would be interesting to confirm the present results using the objects in the deep surveys. We would like to stress that the connection of the opening angle to the fraction of type II ANGs is not firmly sure since the narrow line region in high luminosity quasars may be different from that in Seyfert galaxies (Netzer et al. 2004) and the properties of the highly obscured AGN are not clear (Maiolino et al. 2003). With these uncertainties, the present relation, as a preliminary element, between the Baldwin effect and the evolution of the dusty torus is still robust.

Finally, we like to point out that the presently available data shows only statistically that the origin of the NIKAL is mainly from the dusty torus, however, it might have components from BLR or outer disk region as well. Actually, the scatter in the plot of $EW - L_X$ and $EW - \mathcal{E}$ may be large because of these components of the observed NIKAL EW . The current data does not allow to subtract the component of the NIKAL which originates

from BLR or disk outer region. Future observations of *Astro-E2*, *XEUS* and *Constellation-X* may resolve the different narrow components so that the correlation $EW - \mathcal{E}$ will be improved.

4. CONCLUSIONS

In this paper, we show that the equivalent width of the neutral narrow iron $K\alpha$ line in AGN strongly depends on the Eddington ratio. We exclude the origin from the outer region of the standard accretion disk or self-gravity-dominated disk. The current data statistically supports the origin of this narrow component from the dusty torus. The strong anti-correlation of $EW - \mathcal{E}$ provides a robust probe to the covering factor of the dusty torus.

The most promising explanation of the X-ray Baldwin effect is that it is caused by the evolution of the dusty torus with the hard X-ray luminosity. This is consistent with the population evolution found in the deep surveys of the *Chandra* and *HST*.

The authors are very grateful to an anonymous referee for the very helpful comments improving the paper. T. Rauch is thanked for careful reading of the manuscript. J.M.W. thanks the supports from a Grant for Distinguished Young Scientist from NSFC, NSFC-10233030, the Hundred Talent Program of CAS and the 973 project.

REFERENCES

- Antonucci, R. 1993, *ARA&A*, 31, 473
 Chen, L.-H. & Wang, J.-M., 2004, *ApJ*, 614, 101
 Goodman, J. 2003, *MNRAS*, 339, 937
 Grupe, D., Wills, B. J. et al. 2004, *AJ*, 127, 156
 Hamann F. & Ferland G. 1993, *ApJ*, 418, 11
 Hasinger, G. 2003, astro-ph/0310804
 Immler, S., Brandt, W. N. et al. 2003, *AJ*, 126, 153
 Isobe T., Feigelson E. D., Nelson, P. I. 1986, *ApJ*, 306, 490
 Iwasawa K. & Taniguchi Y. 1993, *ApJ*, 413, 15
 Jaffe, W., Meisenheimer, K. et al. 2004, *Nature*, 429, 47
 Kaspi, S., Smith, P. S., Netzer, H. et al. 2000, *ApJ*, 533, 631
 Krolik, J. H. & Begelman, M. C. 1988, *ApJ*, 329, 702
 Krolik, J. H. & Kallman, T. R. 1987, *ApJ*, 320, 5
 Krolik, J. H., Madau, P. & Zycki, P. T., 1994, *ApJ*, 420, L57
 Lee, J. C., Iwasawa, K., Houck, J. C., et al. 2002, *ApJ*, 570, 47
 Levenson, N. A., et al. 2002, *ApJ*, 573, L81
 Lu, J.-F., Lin, Y.-Q. & Gu, W.-M. 2004, *ApJ*, 602, L37
 Marziani, P.; Sulentic, J. W. et al. 2003, *ApJS*, 145, 199
 Maiolino, R. et al. 2003, *MNRAS*, 344, L59
 Mushotzky, R.; Ferland, G. J. 1984, *ApJ*, 278, 558
 Nandra K., George I. M. et al. 1997, *ApJ*, 488, 91
 Netzer, H. et al. 2004, *ApJ*, 614, 558
 Page, K. L., O'Brien, P. T., et al. 2004, *MNRAS*, 347, 316
 Peterson, B. M., et al. 2004, *ApJ*, 613, 682
 Petrucci P. O., Henri, G. et al. 2002, *A&A*, 388, 5
 Pounds, K. A., Reeves, J. N. et al. 2004, *MNRAS*, 350, 10
 Risaliti, G.; Maiolino, R. et al. 1999, *ApJ*, 522, 157
 Reynolds, C. S., Brenneman, L. W. et al. 2004, *MNRAS*, 352, 205
 Shakura, N. I. & Sunyaev, R. A. 1973, *A&A*, 24, 337
 Shemmer O., Netzer, H. et al. 2004, *ApJ*, 614, 547
 Steffen, A. T., Barger, A. J. et al. 2003, *ApJ*, 596, 23
 Ueda, Y., Akiyama, M. et al. 2003, *ApJ*, 598, 886
 Véron-Cetty, M.-P., Véron, P. 2003, *A&A*, 412, 399
 Vestergaard, M., 2002, *ApJ*, 571, 733
 Wang, J.-M. 2004, *ApJ*, 614, L21
 Wang, J.-M. & Netzer, H. 2003, *A&A*, 398, 927
 Wang, J.-M. & Zhou, Y.-Y. 1999, *ApJ*, 516, 420
 Wilms, J., Reynolds, C. S. et al. 2001, *MNRAS*, 328, 27
 Yaqoob, T., George, I. M. et al. 2001, *ApJ*, 546, 759
 Yaqoob, T., Padmanabhan, U. 2004, *ApJ*, 604, 63

Table 1. The *XMM-Newton* sample of AGNs

Name	z	Type	$\log L_{\text{bol}}$		FWHM	$\log M_{\text{BH}}$		$\log \mathcal{E}$	Ref.	$\log L_X$	$EW_{\text{K}\alpha}$	Ref.
(1)	(2)	(3)	(4)	(5)	(6)	(7)	(8)	(9)	(10)	(11)	(12)	(13)
1H 0707-495	0.0411	NLS1	44.43	R	1050	6.37	R	-0.04	11,13	42.17	< 90	1
I Zw 1 ^b	0.0611	NLS1	45.47	R	1240	7.25	R	0.12	3,13	43.79	34 ± 30	2
Akn 564	0.0247	NLS1	44.21	F	720	6.04	R	0.07	11,13	43.44	< 41	2
IRAS 13224-3809	0.0667	NLS1	45.55	F	650	6.76	R	0.69	11,13	42.95	< 37	2
MCG-5-23-16 ^a	0.0083	NLS1	44.81	R	209	7.85	N	-1.04	7,12	43.02	55 ± 19	2
Mrk 335 ^a	0.0258	NLS1	44.81	R	1629	7.15	M	-0.44	4	43.21	< 54	1
Mrk 359	0.0174	NLS1	43.55	F	480	6.05	R	-0.60	7,8	42.43	220 ± 74	1
Mrk 493	0.0313	NLS1	44.63	F	800	6.32	R	0.21	14	43.14	< 101	1
Mrk 766 ^a	0.0129	NLS1	44.55	F	1360	6.60	R	-0.26	15,14	43.10	45 ± 35	1
Mrk 896	0.0264	NLS1	44.97	F	1135	6.79	R	-1.02	10,15	42.64	180 ± 87	1
Mrk 1044	0.0165	NLS1	44.20	F	1310	6.68	R	-0.58	14,9	42.49	186 ± 61	1
NGC 4051	0.0023	NLS1	42.88	R	1072	6.28	M	-1.50	4	41.39	93 ± 11	2
NGC 5506	0.0062	NLS1	44.02	R	1850	6.30	R	-0.38	7,12	42.77	70 ± 20	1
NGC 7314 ^b	0.0047	NLS1	44.15	R	170	6.70	G	-0.65	5,18	42.22	42 ± 20	2
PG 1211+143 ^a	0.0809	NLS1	45.70	R	1317	8.16	M	-0.56	4	43.57	37 ± 24	1
Ton S180	0.0620	NLS1	45.30	R	980	6.91	R	0.29	13,14	43.56	< 64	1
1H 0419-577	0.1040	BLS1	46.03	F	3460	8.53	R	-0.60	14,16	44.50	< 85	1
3C 120	0.0330	BLS1	45.12	R	2205	7.74	M	-0.72	4	43.91	54 ± 24	2
ESO 198-G24	0.0455	BLS1	45.22	F	6400	8.48	R	-1.36	23,7	43.66	104 ± 49	1
Fairall 9 ^a	0.0470	BLS1	45.20	R	6901	8.41	M	-1.31	4	43.93	139 ± 26	1
IC 4329A	0.0161	BLS1	44.27	R	6431	7.00	M	-0.83	4	44.73	30 ± 12	1
MCG-6-30-15 ^a	0.0077	BLS1	43.59	F	2400	6.30	R	-0.81	13,23	42.84	52 ± 10	1
Mrk 279	0.0305	BLS1	44.83	R	3385	7.54	M	-0.81	4	43.44	71 ± 25	2
Mrk 509 ^a	0.0344	BLS1	45.23	R	2715	8.16	M	-1.03	4	44.62	85 ± 57	1
Mrk 841	0.0364	BLS1	45.64	F	3470	7.90	R	-0.36	3,14	43.83	< 83	1
Mrk 926 ^a	0.0473	BLS1	45.67	F	6300	8.05	R	-0.48	8,15	44.08	< 61	1
NGC 3516 ^{a,b}	0.0088	BLS1	43.84	R	3353	7.63	M	-1.89	4	42.33	196 ± 22	1
NGC 3783	0.0097	BLS1	44.21	R	3093	7.47	M	-1.36	4	42.96	120 ± 14	2
NGC 4151	0.0033	BLS1	43.83	R	4248	7.12	M	-1.39	4	42.21	187 ± 3	1
NGC 4593	0.0090	BLS1	44.04	R	3769	6.73	M	-0.79	4	43.02	98 ± 21	1

Table 1—Continued

Name	z	Type	$\log L_{\text{bol}}$		FWHM	$\log M_{\text{BH}}$		$\log \mathcal{E}$	Ref.	$\log L_X$	$EW_{\text{K}\alpha}$	Ref.
(1)	(2)	(3)	(4)	(5)	(6)	(7)	(8)	(9)	(10)	(11)	(12)	(13)
NGC 5548	0.0172	BLS1	44.46	R	4044	7.83	M	−1.47	4	43.33	59 ± 6	1
NGC 7213 ^b	0.0060	BLS1	44.30	I	3200	7.99	R	−1.79	11,17	42.21	82 ± 16	2
NGC 7469	0.0163	BLS1	44.70	R	2169	7.09	M	−0.49	4	43.11	105 ± 25	2
PG 0844+349 ^a	0.0640	BLS1	45.30	R	2148	7.97	M	−0.77	4	43.82	< 172	1
3C 273	0.1583	RLQ	47.03	R	3520	8.82	R	0.11	3	45.66	< 9	1
III Zw 2	0.0898	RLQ	45.81	R	3980	8.29	R	−0.58	3,11	44.28	< 84	1
B2 1028+31 ^a	0.1782	RLQ	-	-	-	-	-	-	-	44.20	88 ± 41	1
B2 1128+31 ^a	0.2890	RLQ	46.05	R	3400	8.44	R	−0.49	15,11	44.66	50 ± 39	1
B2 1721+34	0.2060	RLQ	46.22	R	3450	8.72	R	−0.60	15,11	44.84	63 ± 34	1
HE 1029-1401	0.0860	RQQ	45.95	R	7400	8.73	R	−0.88	15,11	44.48	< 105	1
MR 2251-178	0.0640	RQQ	45.40	R	4800	8.01	R	−0.71	6,15	44.40	< 74	1
Mrk 205 ^a	0.0708	RQQ	45.85	R	3150	8.32	R	−0.57	6,15	43.89	60 ± 25	1
Mrk 304	0.0658	RQQ	45.42	R	6170	7.91	R	−0.59	11,24	43.76	< 115	1
Mrk 876	0.1290	RQQ	45.60	F	8450	8.88	R	−1.38	3,14	44.13	96 ± 59	1
Mrk 1383	0.0865	RQQ	45.78	R	5940	8.75	R	−1.07	3,11	44.04	77 ± 46	1
NGC 3227	0.0039	RLQ	43.33	R	5138	7.63	M	−2.40	4	41.33	191 ± 23	1
PB 05062	1.7700	RQQ	-	-	-	-	-	-	-	46.80	< 61	1
PDS 456	0.1840	RQQ	46.90	R	3010	8.91	R	−0.11	6,22	44.71	< 18	1
PG 0804+761 ^a	0.1000	RQQ	45.89	R	2012	8.84	M	−1.07	4	44.26	< 101	1
PG 0947+396	0.2060	RQQ	45.89	R	4830	8.72	R	−0.93	21	44.17	93 ± 65	2
PG 1048+342	0.1670	RQQ	45.51	R	3890	8.26	R	−0.85	11,15	44.15	< 191	1
PG 1114+445	0.1440	RQQ	45.65	R	4570	8.41	R	−0.86	3,6	44.21	120 ± 17	1
PG 1309+355 ^a	0.1840	RLQ	45.82	R	2940	8.26	R	−0.54	21	43.66	< 236	2
PG 1411+442	0.0896	RQQ	45.58	R	2398	8.65	M	−1.17	4	43.54	290 ± 132	2
PG 1512+370	0.3707	RLQ	46.36	R	6810	9.14	R	−0.88	21	44.72	63 ± 54	2
PG 1626+554	0.1330	RQQ	45.67	F	4490	8.50	R	−0.93	14,21	44.32	< 281	1
PG 1634+706	1.3340	RQQ	-	-	-	-	-	-	-	46.05	< 63	1
PKS 0438-43	2.8630	RLQ	-	-	-	-	-	-	-	46.85	< 26	1
PKS 0537-286	3.1040	RLQ	47.60	R	12130 ^c	9.65	S	−0.15	6,20	47.37	< 82	1
PKS 1637-77	0.0427	RLQ	-	-	-	-	-	-	-	43.67	< 95	1

Table 1—Continued

Name	z	Type	$\log L_{\text{bol}}$		FWHM	$\log M_{\text{BH}}$		$\log \mathcal{E}$	Ref.	$\log L_X$	$EW_{\text{K}\alpha}$	Ref.
(1)	(2)	(3)	(4)	(5)	(6)	(7)	(8)	(9)	(10)	(11)	(12)	(13)
PKS 2149-306	2.3450	RLQ	47.51	R	6400 ^c	9.50	S	-0.09	6,20	46.97	< 40	1
Q 0056-363 ^a	0.1620	RQQ	46.30	R	4550	8.95	R	-0.75	14,11	44.17	< 159	1
Q 0144-3938	0.2440	RQQ	-	-	-	-	-	-	-	44.28	152 ± 50	1
S5 0014+81	3.3660	RLQ	-	-	-	-	-	-	-	47.14	< 17	1
S5 0836+71	2.1720	RLQ	-	-	-	-	-	-	-	47.63	16 ± 6	1
UM 269	0.3084	RQQ	-	-	-	-	-	-	-	44.40	< 99	1

Note. — (1): source name, (2): redshift, (3): type, (4): bolometric luminosity (erg s^{-1}), (5): Note on method for estimates of bolometric luminosity. R: relation of $L_{\text{bol}} = 9\lambda L_{\lambda}(5100\text{\AA})$ (K00, Netzer 2003); F: spectral energy distribution fitting; I: flux integration, (6): FWHM $\text{H}\beta$ (km s^{-1}), (7): black-hole mass (M_{\odot}), (8): note on method for estimates of black-hole masses, M: reverberation mapping measurement; R: the empirical reverberation relation; S: Single-epoch mass determination method, $M_{\text{BH}} = 1.6 \times 10^6 (\lambda L_{\lambda,44}(1350\text{\AA}))^{0.7} (V_{\text{FWHM}\text{Civ},3})^2 M_{\odot}$ (V02); N: relation for narrow line region size, $R_{\text{NLR}} = 1.15 L_{\text{H}\beta,42}^{0.49}$ kpc (Netzer et al. 2004); V: measurements of the central velocity gradient, taken from Schulz et al. (1994), (9): Eddington ratio, $\mathcal{E} = L_{\text{bol}}/(1.26 \times 10^{38} M_{\text{BH}})$, (10): reference for optical data, (11): the X-ray luminosity in the rest frame 2 – 10 keV band (erg s^{-1}), (12): the rest frame Equivalent Width of neutral narrow Fe $\text{K}\alpha$ line at 90% error confidence(eV). The *XMM-Newton* PN data only are used. As described in P04, the spectral fittings are performed via a model of a simple power law over the rest frame band of 2 - 10 keV modified by the Fe K edge. If there was evidence for the emission of broad line, a broad Gaussian model is included. Then a narrow Gaussian (the intrinsic width is fixed at 10 eV) is added for the EW measurements. The neutral reflection component (PEXRAV in XSPEC, see Magdziarz & Zdziarski 1995) is also tried for each spectrum. (13): reference for X-ray data

References. — 1: Page et al. (2004); 2: this work; 3: Vestergaard et al. (2002); 4: Peterson et al. (2004); 5: Schulz et al. (1994); 6: Reeves & Turner (2000) 7: Whittle (1992); 8: Osterbrock et al. (1982); 9: Rafanelli et al. (1983); 10: Veilleux (1991); 11: Véron-Cetty et al. (2003); 12: Wilson et al. (1985); 13: Turner et al. (1999); 14: Grupe et al. (2004); 15: Marziani et al. (2003); 16: Guainazzi et al. (1998) 17: Woo & Urry (2002); 18: Padovani et al. (1988) 19: Vaughan et al. (1999); 20: Wilkes (1986); 21: Porquet et al. (2004); 22: Reeves et al. (2000a); 23: Winkler (1992); 24: Condon et al. (1985)

^aBroad line is statistically required in the rest frame band of 2 – 10 keV

^bMultiple narrow Gaussians in the rest-frame band of 2 – 10 keV

^cFull width at half maximum of the C IV line (1549 \AA)

REFERENCES

- Condon, J. J. et al. 1985, *AJ*, 90, 1642 2003, *A&A*, 405, 909
- Gallo, L. C., Boller Th. et al. 2004, *A&A*, 417, 29
- Grupe, D., Wills, B. J. et al. 2004, *AJ*, 127, 156
- Guainazzi, M., Comastri, A., et al. 1998, *A&A*, 339, 327
- Magdziarz P. & Zdziarski A.A., 1995, *MNRAS*, 273, 837
- Marziani, P. & Sulentic, J. W. et al. 2003, *ApJS*, 145, 199
- Netzer, H., 2003, *ApJ*, 583, L5
- Netzer, H., Shemmer, O. et al. 2004, *ApJ*, in press, astro-ph/0406560
- Osterbrock, D. E. & Shuder, J. M. 1982, *ApJS*, 49, 149
- Padovani, P., Rafanelli, P. 1988, *A&A*, 389, 802
- Page, K. L., O'Brien, P. T. et al. 2004, *MNRAS*, 347, 316
- Peterson, B. M., Ferrarese, L. et al. 2004, *ApJ*, in press, astro-ph/0407299
- Rafanelli, P. & Schulz, H. 1983, *A&A*, 117, 109
- Reeves, J. N., O'Brien, P. T. et al. 2000a, *MNRAS*, 312, 17
- Reeves, J. N. & Turner M. J. L. 2000b, *MNRAS*, 316, 234
- Schulz, H., Knake, A. et al. 1994, *A&A*, 288, 425
- Turner, T. J., George, I. M. et al. 1999, *ApJ*, 524, 667
- Vaughan, S., Reeves, J. et al. 1999, *MNRAS*, 309, 113
- Veilleux, S. 1991, *ApJS*, 75, 383
- Véron-Cetty, M.-P., Véron, P. 2003, *A&A*, 412, 399
- Vestergaard, M., 2002, *ApJ*, 571, 733
- Whittle, M. 1992, *ApJS*, 79, 49
- Wilson, A. S., Baldwin, J. A. et al. 1985, *ApJ*, 291, 627

Wilkes, B. J. 1986, MNRAS, 218, 331

Winkler, H. 1992, MNRAS, 257, 677

Woo, J. H. & Urry, C. M. 2002, ApJ, 579, 530